VLT spectroscopy of GRB 990510 and GRB 990712; probing the faint and bright ends of the GRB host galaxy population

Vreeswijk, P.M.; Fruchter, A.; Kaper, L.; Rol, E.; Galama, T.J.; van Paradijs, J.A.; Kouveliotou, C.; Wijers, R.A.M.J.; Pian, E.; Palazzi, E.; Masetti, N.; Frontera, F.; Savaglio, S.; Reinsch, K.; Hesman, F.V.; Beuermann, K.; Nicklas, H.; van den Heuvel, E.P.J.

Published in:
Astrophysical Journal

DOI:
10.1086/318308

THE ASTROPHYSICAL JOURNAL, 546:672–680, 2001 January 10

VLT SPECTROSCOPY OF GRB 990510 AND GRB 990712: PROBING THE FAINT AND BRIGHT ENDS OF THE GAMMA-RAY BURST HOST GALAXY POPULATION[1]

P. M. VREESWIJK,[2] A. FRUCHTER,[3] L. KAPER,[2] E. ROL,[2] T. J. GALAMA,[4] J. VAN PARADIJS,[2,5,6] C. KOUVELIOTOU,[7,8] R. A. M. J. WIJERS,[9] E. PIAN,[10] E. PALAZZI,[10] N. MASETTI,[10] F. FRONTERA,[10,11] S. SAVAGLIO,[3,12,13] K. REINSCH,[14] F. V. HESSMAN,[14] K. BEUERMANN,[14] H. NICKLAS,[14] AND E. P. J. VAN DEN HEUVEL[2]

Received 2000 June 14; accepted 2000 August 31

ABSTRACT

We present time-resolved optical spectroscopy of the afterglows of the gamma-ray bursts GRB 990510 and GRB 990712. Through the identification of several absorption lines in the first-epoch GRB 990510 spectrum, we determine the redshift for this burst at $z \geq 1.619$. No clear emission lines are detected. The strength of the Mg I feature is indicative of a dense environment, most likely the host galaxy of GRB 990510. Although the host is extremely faint ($V \gtrsim 28$), the GRB afterglow allows us to probe its interstellar medium and—in principle—to measure its metallicity. The optical spectrum of GRB 990712 (whose host galaxy is the brightest of the known GRB hosts at cosmological redshifts) shows clear features both in emission and absorption, at a redshift of $z = 0.4331 \pm 0.0004$. On the basis of several line emission diagnostic diagrams, we conclude that the host galaxy of GRB 990712 is most likely an H II galaxy. We derive an unreddened [O II] star formation rate of $2.7 \pm 0.8\ M_{\odot}\ \mathrm{yr}^{-1}$. Correcting for the measured extinction intrinsic to the host galaxy ($A_V = 3.4^{+2.4}_{-1.7}$), this value increases to $35^{+178}_{-25}\ M_{\odot}\ \mathrm{yr}^{-1}$. The [O II] equivalent width, compared to that of field galaxies at $z \leq 1$, also suggests that the host of GRB 990712 is vigorously forming stars. We employ the oxygen and Hβ emission-line intensities to estimate the global oxygen abundance for the host of GRB 990712: $\log(\mathrm{O/H}) = -3.7 \pm 0.4$, which is slightly below the lowest metallicity one finds in nearby spiral galaxies. For both GRBs we study the time evolution of the absorption lines, whose equivalent width might be expected to change with time if the burst resides in a dense compact medium. We find no evidence for a significant change in the Mg II width.

Subject headings: cosmology: observations — galaxies: distances and redshifts — galaxies: starburst — gamma rays: bursts

1. INTRODUCTION

In 1997 February, the Italian-Dutch satellite *BeppoSAX* enabled a breakthrough in the understanding of gamma-ray bursts (GRBs) by providing an accurate position for the prompt X-ray emission of a GRB. This led to the discovery of the first X-ray afterglow of a GRB (Costa et al. 1997) and, independently, to the identification of the first optical counterpart of a burster (van Paradijs et al. 1997). Since then, several X-ray, optical, and radio counterparts of GRBs have been detected. These multiwavelength afterglow observations can be explained reasonably well by simple fireball models (for recent reviews see Piran 1999; van Paradijs, Kouveliotou, & Wijers 2000). GRB distance determinations are crucial in the effort to establish the physical nature of their progenitor(s). The observed redshift distribution of the "normal" afterglows (i.e., excluding GRB 980425, which is associated with supernova SN 1998bw at $z = 0.0085$; Galama et al. 1998) ranges from $z = 0.43$ (Galama et al. 1999; this paper) to $z = 3.42$ (Kulkarni et al. 1998).

Although major advances in the understanding of GRBs have been made over the past few years (thanks to the detection of afterglows), the physical nature of their progenitor(s) remains unclear. The most popular models are (1) the collapse of a rotating massive star (Woosley 1993; MacFadyen & Woosley 1999) and (2) the merging of two neutron stars or a neutron star and a black hole (Narayan, Paczyński, & Piran 1992; Janka et al. 1999). The former ("collapsar") model has trouble producing GRBs with durations shorter than a couple of seconds and predicts that every afterglow is accompanied by a supernova of a type (Ic) similar to SN 1998bw (MacFadyen & Woosley 1999). Furthermore, in the collapsar environment it is likely that the optical light of the afterglow is heavily absorbed by the surrounding dusty medium. Given the massive progenitors, one expects the frequency of GRBs to be strongly correlated with the cosmic star formation rate; the latter remains one

[1] Based on observations collected at the European Southern Observatory, Chile; proposal 63.O-0567.

[2] Astronomical Institute "Anton Pannekoek," University of Amsterdam and Center for High Energy Astrophysics, Kruislaan 403, 1098 SJ Amsterdam, Netherlands.

[3] Space Telescope Science Institute, 3700 San Martin Drive, Baltimore, MD 21218.

[4] California Institute of Technology, 1200 East California Boulevard, Pasadena, CA 91125.

[5] Physics Department, University of Alabama in Huntsville, Huntsville, AL 35899.

[6] Deceased.

[7] Universities Space Research Association.

[8] NASA/MSFC, Code SD-50, Huntsville, AL 35812.

[9] Department of Physics and Astronomy, SUNY Stony Brook, Stony Brook, NY 11794-3800.

[10] ITESRE-CNR Bologna, Via P. Gobetti 101, 40129 Bologna, Italy.

[11] Physics Department, University of Ferrara, Via Paradiso, 12, 44100 Ferrara, Italy.

[12] On assignment from the Space Science Department of the European Space Agency.

[13] Currently at the Observatory of Rome, via di Frascati 33, I-00040 Monteporzio Catone, Italy.

[14] Universitäts-Sternwarte, Geismarlandstrasse 11, D-37083 Göttingen, Germany.

of the great unresolved issues in astronomy of today. The compact star merger scenario can make short GRBs as well as long ones (although a 10^{15} G magnetic field is probably needed for the latter; see Mészáros 2000); some of these mergers are expected to occur in low-density environments, possibly located several kiloparsecs outside their host galaxies. This is due to the large kick velocities imparted to the compact objects from the two respective supernovae ($\sim$250–300 km s^{-1}; Hansen & Phinney 1997), combined with the long time between the birth of the system and the merger occurrence (10^8–10^9 yr; Portegies Zwart & Yungelson 1998). Consequently, since the optical afterglow brightness depends on the density of the circumsource medium, some of these bursts may not show an afterglow at all. These could account for the "dark" burst population, i.e., bursts for which only X-ray afterglows have been found. One way to discriminate between these two models is by studying the immediate environment of the burst. In the collapsar model the circumsource density is expected to drop with distance as r^{-2}, due to the expanding stellar wind of the supernova (SN) progenitor, while in the binary merger scenario a constant, relatively low-density ambient medium is most plausible.

If the GRB source resides in a compact, gas-rich environment (which is expected in the collapsar scenario), the afterglow spectrum might show time-dependent absorption features (such as Lyα and Mg II) due to the gradual ionization of the surrounding medium (Perna & Loeb 1998). In this case a decrease of the absorption-line equivalent widths (EWs) with time is expected. On the other hand, spectroscopic observations of the star HD 72089, situated behind the Vela supernova remnant, show an increase of an order of magnitude of the absorption strengths of elements such as Al and Fe, over the velocity range spanned by absorption in the remnant (Jenkins & Wallerstein 1995; see also Savage & Sembach 1996). This is attributed to the destruction of the dust grains, due to the propagation of the SN shock, which causes the release of elements (such as Fe and Mg) that are frozen in the dust. Thus, in a dusty environment that is being "shocked" by a GRB explosion, one might expect the strength of the absorption lines to increase in time.

In order to test these theories of GRB genesis, and the effects of GRBs on their environments, we have an ongoing program to obtain spectra of GRB afterglows using the Very Large Telescope (VLT) of the European Southern Observatory (ESO) at Paranal, Chile. Here we present results on two of these bursts: GRB 990510 and GRB 990712.

1.1. *GRB 990510*

GRB 990510 was observed on 1999 May 10.36743 UT with the Wide Field Camera (WFC) unit 2 on board *BeppoSAX*, which localized the burst at R.A. = $13^h38^m06^s$, Decl. = $-80°29'30''$ (J2000.0), with an error radius of $3'$ (Dadina et al. 1999). The *BeppoSAX* Gamma Ray Burst Monitor (GRBM) recorded an 80 s event with a multipeak structure (40–700 keV). The average and peak intensity in the WFC unit 2 (2–28 keV) was about 0.7 and 4.3 crab, respectively. The burst position as determined with *BeppoSAX* is consistent with that of the Interplanetary Network (IPN) (Hurley et al. 1999), using the Burst and Transient Source Experiment (BATSE) on board the *Compton Gamma Ray Observatory*, and *Ulysses*. BATSE recorded a fluence above 20 keV of 2.56×10^{-5} ergs cm^{-2} (Kippen et al. 1999), ranking it in the top 9% of the burst fluence distribution.

We discovered the optical afterglow on images taken at the South African Astronomical Observatory (SAAO) 1 m telescope (Vreeswijk et al. 1999) and subsequently triggered our VLT program to take spectra and polarimetric images. Here we present the time-resolved spectroscopy. Our polarimetric observations resulted in the first polarization detection of a GRB afterglow (Wijers et al. 1999; see also Covino et al. 1999), while our photometric observations show an achromatic break in the *BVRIJHK* light curves, which is most likely due to the burst emission being collimated (E. Rol et al. 2000, in preparation; see also Stanek et al. 1999; Harrison et al. 1999). Fruchter et al. (1999) have used the *Hubble Space Telescope* (*HST*) to estimate $V_{\rm host} \gtrsim 28$ and do not find evidence for a supernova of the same type and brightness as SN 1998bw in the late-time light curve of GRB 990510. Recent *HST* observations (2000 April) appear to detect a faint galaxy ($V \sim 28$) at the position of the early optical transient, which, if real, is most likely the host of GRB 990510 (Fruchter et al. 2000; Bloom et al. 2000).

1.2. *GRB 990712*

GRB 990712 triggered the GRBM and WFC unit 2 on board *BeppoSAX* on 1999 July 12.69655 UT. The burst lasted for about 30 s, had a double-peaked structure, was moderate in gamma rays, and was accompanied by one of the strongest prompt X-ray counterparts ever observed (Heise et al. 1999). The WFC unit 2 located the burst at R.A. = $22^h31^m50^s$, Decl. = $-73°24'24''$ (J2000.0), with an error radius of $2'$. Unfortunately, neither flux nor fluence levels are reported in the literature. Again the SAAO 1 m telescope was successful in hunting down the GRB afterglow (Bakos et al. 1999), which allowed us to quickly alert the VLT staff for spectroscopic, polarimetric, and further photometric follow-up observations. The host galaxy of GRB 990712 is the brightest of the known GRB host galaxies, with $R = 21.8$ and $V = 22.3$ (Sahu et al. 2000). The VLT polarimetric images exhibit a significant degree of polarization of the afterglow of GRB 990712 which seems to vary with time, while the polarization angle does not change with time (Rol et al. 2000). These observations cannot be easily reconciled with afterglow polarization theories. The photometric measurements show a common temporal power-law decay of the transient source, overtaken by the bright host galaxy at late times; no evidence is found for a supernova of type SN 1998bw (Sahu et al. 2000; see also Hjorth et al. 2000).

The organization of this paper is as follows. In § 2 we present the observations and data reduction methods. In § 3 we display and discuss the spectra of GRB 990510, followed by GRB 990712 in § 4. We study the absorption-line intensity evolution in time for both bursts in § 5 and describe our conclusions in § 6.

2. OBSERVATIONS

After the optical identification of both GRB 990510 (Vreeswijk et al. 1999) and GRB 990712 (Bakos et al. 1999), we triggered our VLT target-of-opportunity observation program and obtained several low-resolution spectra at various epochs with the focal reducer and low-dispersion spectrograph (FORS), mounted at the Cassegrain focus of the ESO VLT-UT1 Antu telescope. The date of obser-

vation, grism used, wavelength range, resolving power, and the signal-to-noise ratio at 6500 Å are listed in Table 1. A slit width of 1″ was used for all spectra. Grism G150I approximately covers the wavelength range 3700–9000 Å. However, redward of 6500 Å the second order starts to contaminate the first order (cf. FORS User Manual 1.3). To obtain a clean spectrum longward of 6500 Å for GRB 990510, we also took spectra with an order separation filter (OG590), using the same grism. However, due to the low sensitivity of the CCD shortward of 3700 Å, the impact of the overlap is negligible shortward of 7700 Å. Therefore, we have summed the blue and red spectra over the region 6200–7700 Å and combined this part with the single blue and red spectra into a continuous spectrum over the entire wavelength range. For the grisms G300V and G300I, we have simply connected the blue and red parts into one spectrum. For GRB 990712, we used grism G150I without order separation filter, and thus these spectra are usable over the wavelength range 3700–7700 Å.

The raw spectra were bias subtracted and flat-fielded with a normalized combined set of lamp flat fields. Subsequently, cosmic rays were removed interactively along the afterglow spectrum, and each sequence of images was summed into combined images. The spectra were optimally extracted from the combined images and wavelength calibrated using a standard helium-neon-argon lamp. The rms error in the wavelength calibration is approximately 0.25 Å. Since no useful spectra of standard stars were taken either during the first two nights for GRB 990510 or for GRB 990712, we have flux calibrated these spectra using the *BVRI* light curve data of E. Rol et al. (2000, in preparation) for GRB 990510 and the VRI data of Sahu et al. (2000) for GRB 990712. The spectra of the other nights were flux calibrated with a spectrophotometric standard star, which resulted in flux levels that are consistent with the photometry at the same epochs.

To flux calibrate the spectrum of GRB 990510, we fitted the light curves with a smoothly connected broken power-law model (Harrison et al. 1999; Stanek et al. 1999; Beuermann et al. 1999), while for GRB 990712 we used a simple power-law model with a host galaxy contribution. We determined the magnitudes at the times when the spectra were taken (see Table 1), using the fits to the light curves. These values were then corrected for the estimated Galactic foreground extinction: $E(B-V) = 0.2$ and $E(B-V) = 0.03$ (Schlegel, Finkbeiner, & Davis 1998) for the May and July burst, respectively. The $E(B-V)$ value is translated into an extinction at a given wavelength using the standard Galactic extinction curve of Cardelli, Clayton, & Mathis (1989). The magnitudes were transformed to fluxes (Fukugita, Shimasaku, & Ichikawa 1995) and were fitted with a power-law spectrum $F \propto \nu^{\beta}$. For GRB 990510 we find $\beta = -0.6 \pm 0.1$ (first night) and $\beta = -0.7 \pm 0.1$ (second night). For the three spectra of GRB 990712 we obtain $\beta(1) = -1.1 \pm 0.2$, $\beta(2) = -0.9 \pm 0.2$, and $\beta(3) = -0.9 \pm 0.2$. We have not taken into account the extinction intrinsic to the host galaxy; see § 4. These slopes are quite usual for GRB afterglows. We also fitted the global profile (excluding the absorption and emission lines) of all the wavelength-calibrated spectra with a fourth-order Chebyshev polynomial. To obtain the flux-calibrated spectra, we multiplied the wavelength-calibrated spectra by the ratio between the power-law fit based on the photometry and the global spectral profile fit. We estimate the error in the flux calibration for all nights to be about 15%.

The equivalent width (EW) of the spectral lines was measured using the SPLOT routine in IRAF; we used a Gaussian fit and also simply summed the difference between the pixel value and the continuum for each pixel over the line. Both methods gave similar results. The error is mostly dominated by the uncertainty in the continuum level, which was estimated by placing the continuum at a high and low level (roughly corresponding to the $\pm$rms value of the continuum in the vicinity of the line). We take the mean value of these two estimates as the EW and half their difference as the error. We also calculate the Poisson error from the object and sky spectrum, which we quadratically sum with the measurement error to obtain the total error. We then corrected the EW for the host galaxy contribution in case of absorption features (i.e., divided the measured EW by the afterglow fraction of the total light) and for the afterglow contribution in case of an emission line (i.e., divided by the galaxy-light fraction of the total). The host galaxy fraction of the total light for GRB 990510 is negligible (see § 3), while for GRB 990712 we obtain 0.23 ± 0.03, 0.30 ± 0.04, and 0.47 ± 0.06 for epochs one, two, and three, respectively, from the *V*- and *R*-band light curve fits of Sahu et al. (2000). The error was estimated from the different values for the host galaxy magnitude as given by Sahu et al. (2000) and Hjorth et al. (2000). These errors are propagated along with the errors in the EW measurements. Finally, the EW is converted to the rest frame by dividing by $(1 + z)$. The

TABLE 1

Log of the GRB 990510 and GRB 990712 Spectroscopic Observations

UT Date (1999)	Time Since Burst (days)	Grism	Wavelength Range (Å)	Resolving Power	S/N at 6500 Å
GRB 990510:					
May 11.179.....	0.811	G150I	3700–7700	185	91
May 11.203.....	0.836	G150I + OG590	6000–9000	280	78
May 12.123.....	1.755	G150I	3700–7700	185	6
May 12.146.....	1.779	G150I + OG590	6000–9000	280	6
May 14.273.....	3.906	G300V and G300I	3880–9255	420 and 680	9
May 16.254.....	5.887	G150I	3700–7700	185	5
GRB 990712:					
July 13.182	0.485	G150I	3700–7700	185	26
July 13.421	0.725	G150I	3700–7700	185	21
July 14.181	1.485	G150I	3700–7700	185	14

Note.—The total exposure time for all spectra was 1800 s.

emission-line fluxes are independent of the afterglow contribution to the total light.

3. THE ABSORPTION-LINE SPECTRUM OF GRB 990510

We have identified several absorption lines in the first-epoch spectrum of GRB 990510: Mg II λ2800; Mg I λ2853; Fe II $\lambda\lambda$2344, 2383, 2600; and possibly Al III λ1683 and Cr II/Zn II λ2062. The observed wavelengths, identifications, corresponding redshifts, and equivalent widths (in the absorber's rest frame) are listed in Table 2. The lines and the telluric absorption features are also indicated in Figure 1.

These line identifications can be verified by taking into account the oscillator strength, ionization potential, and relative cosmic abundance. The observed EWs of Fe II at 2344, 2383, and 2600 Å are in reasonable agreement with their relative oscillator strengths (Morton 1991). Other Fe II lines, such as Fe II λ1608 and Fe II λ2587, were not observed, but these have smaller oscillator strengths, consistent with their nondetection. However, the oscillator strength of the undetected Al III λ1855 is twice that of the detected Al III λ1863 line and so should have been detected at an observed wavelength of 4858 Å. This makes the identification of the line at 4883 Å with Al III questionable. A similar argument can be made for the reality of the Cr II/Zn II λ2062 line. Both lines are expected to be accompanied by a stronger partner (Cr II λ2056 and Zn II λ2026), which is not detected. The presence of Fe II suggests that the medium probed with our line of sight is most likely one of low ionization, and there-

TABLE 2

ABSORPTION LINES IN GRB 990510

λ_{obs} (Å)	Identification	z_{abs}	$W_{\lambda,rest}$ (Å)
4883 ± 6	Al III (λ1862.79)?	1.6213 ± 0.0032	0.8 ± 0.6 (0.010)
5396 ± 5	Cr II (λ2062.23)/Zn II (λ2062.66)?	1.6166 ± 0.0024	0.8 ± 0.3 (0.010)
6142 ± 3	Fe II (λ2344.21)	1.6201 ± 0.0013	0.6 ± 0.2 (0.011)
6241 ± 5	Fe II (λ2382.76)	1.6192 ± 0.0021	0.5 ± 0.3 (0.012)
6806 ± 3	Fe II (λ2600.17)	1.6175 ± 0.0011	0.9 ± 0.2 (0.011)
7335 ± 2	Mg II (λ2796.35/λ2803.53)	1.6197 ± 0.0034	2.6 ± 0.4 (0.017)
7472 ± 6	Mg I (λ2852.96)	1.6190 ± 0.0021	0.6 ± 0.2 (0.013)
Weighted mean.....		1.6187 ± 0.0015	

NOTES.—W_λ is given in the absorber's rest frame, i.e., the observed value is divided by $(1 + z)$. The error in W_λ is dominated by the uncertainty in the placing of the continuum. The relative error expected from Poisson statistics and read noise is given in parentheses. The weighted mean redshift is calculated, using the separate measurements of all the lines, even though the identification of Al III and Cr II/Zn II is uncertain (see text).

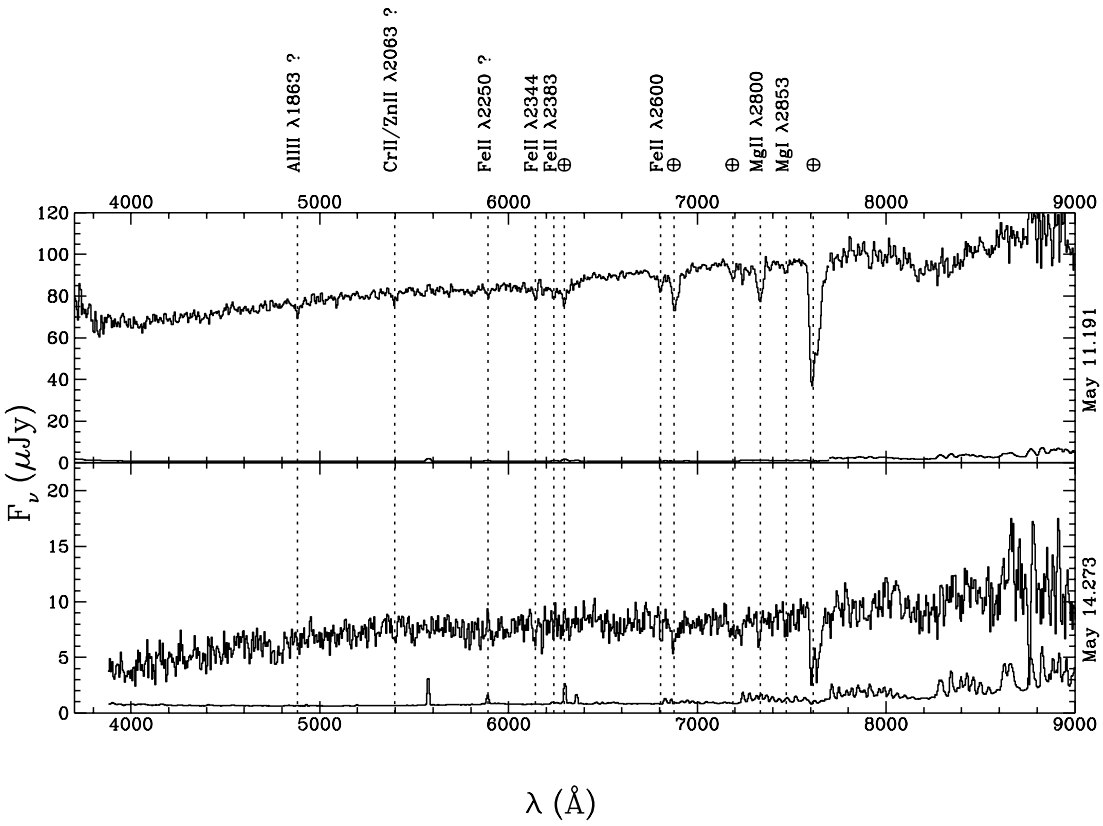

FIG. 1.—VLT/FORS1 spectra of the afterglow of GRB 990510: 0.8 and 3.9 days after the burst. The error spectra, calculated from the object and sky spectra using Poisson statistics, are also shown. Several absorption features (including telluric lines marked with ⊕) are indicated with the broken lines.

fore Al II λ1670 is expected to be present as well given the similarity between the Fe and Al ionization potentials, but again nothing is detected. However, we clearly detect Mg II, which is a blend of Mg II λ2796 and Mg II λ2804, and observe Mg I λ2853 in absorption as well.

The weighted mean redshift of the identified lines is $z = 1.6187 \pm 0.0015$. On the basis of this redshift we can possibly identify Fe II (λ2250) at 5893 Å, although we do not expect to detect this line due to its low oscillator strength. Since no clear emission lines are detected, this redshift is certainly a lower limit to the redshift of the GRB afterglow. However, the strength of Mg I λ2853 suggests we are probing a dense, low-ionization medium, very likely that of the host galaxy. Assuming isotropic emission, $z = 1.619$, $H_0 = 70$ km s^{-1} Mpc^{-1}, $\Omega_0 = 0.3$, and $\Lambda = 0$, we find a luminosity distance of 3.5×10^{28} cm, corresponding to an (>20 keV) energy output of 1.5×10^{53} ergs for GRB 990510, based on the BATSE fluence of 2.56×10^{-5} ergs cm^{-2} (Kippen et al. 1999; see also Briggs et al. 2000).

Unfortunately, the spectra taken on May 12 and May 16 (not shown in Fig. 1) are of inferior quality and cannot be used for absorption-line measurements. In the May 14 spectrum, however, we detect Mg II again. The observed wavelength of $\lambda_{\rm obs} = 7327 \pm 5$ Å is consistent with the redshift determined in the first-epoch spectrum. Its equivalent width is $W_{\rm rest} = 2.3 \pm 0.6$ Å, which is (within the errors) identical to the measurement of 1999 May 11.2 UT (0.8 days after the burst; $W_{\rm rest} = 2.6 \pm 0.4$ Å). For the other absorption lines detected earlier, it is not possible to obtain an accurate measurement of their EWs.

We will now derive a lower limit to the H I column in the direction of GRB 990510 from the Fe II lines at 2344, 2600, and 2383 Å in the first-epoch spectrum. The relation among the EW of a line, W_λ, its column density, N_j (number of atoms in the corresponding ionization state), and the oscillator strength, f, of the transition (j) is (Spitzer 1978)

$$\log (W_\lambda/\lambda) = \log (N_j \times \lambda \times f) - 4.053 \ .$$

Here the unit of W_λ is Å, the column density N_j is in cm^{-2}, and the wavelength λ is in cm. We do not use the strongest absorption line, Mg II λ2800, since this line is easily saturated in typical galaxy spectra, placing it on the flat part of the curve of growth (W_λ vs. $N_j \times \lambda \times f$). Even if the error in the EW determination were very small, this would still lead to a very uncertain value for the column density. The Mg I line is not used either, due to the large uncertainty in the ratio of Mg I to Mg II, translating in a similar uncertainty in the column density. Fe II, however, should be the dominant Fe ion in a dense neutral environment. The following holds if the Fe lines are not saturated. Using the oscillator strength values from Morton (1991) for these lines [f(Fe II λ2344) = 0.110, f(Fe II λ2383) = 0.301, and f(Fe II λ2600) = 0.224], and the values for W_λ obtained from the spectrum of the first epoch (see Table 2), we obtain $\log N$(Fe II λ2344) = 14.0 ± 0.1 cm^{-2}, $\log N$(Fe II λ2383) = 13.5 ± 0.2 cm^{-2}, and $\log N$(Fe II λ2600) = 13.8 ± 0.1 cm^{-2}. We adopt the value $\log N$(Fe) = 13.8 ± 0.2 cm^{-2}. Even though the EWs of the three different Fe lines result in similar values for the column, the lines are probably saturated; i.e., our estimate for the Fe column density should be considered as a lower limit.

In converting the number of Fe atoms to a hydrogen column density, we have to take into account that the metallicity in high-redshift galaxies is likely to be lower than the Galactic value and that a large fraction of the Fe atoms can be hidden in dust (Whittet 1992). A study of the metallicity in damped Lyα systems [which have N(H I) $\gtrsim 10^{20}$ cm^{-2}] from $z = 0.7$ to 3.4 (Pettini et al. 1997; we adopt [Zn/H] = -0.8) allows us to estimate the Fe abundance at the redshift of GRB 990510 with respect to the solar abundance (Grevesse & Sauval 1999; $\log$ (Fe/H)$_\odot = -4.5$), obtaining $\log \{N({\rm Fe})/N({\rm H})\} = -5.3$. The Galactic Fe depletion factor in a cool disk environment is -2.2 dex (Sembach & Savage 1996; Savage & Sembach 1996), but here we adopt the typical depletion measured in damped Lyα systems, which is around -0.6 dex. Taking all these points into account gives the following rough lower limit to the hydrogen column density: $\log N$(H I) ≥ 19.7 cm^{-2}. Another and more robust way of estimating the H I column density which is independent of dust corrections is to use the Fe II measured in damped Lyα absorbers (DLAs) (the gas phase only) around the redshift of the GRB. Using 10 systems with redshifts ranging from 1.2 to 2.0, we find [Fe/H] = -1.5 ± 0.5. Assuming that this is the most likely [Fe/H] abundance for the host galaxy of GRB 990510, we obtain $\log N$(H I) $\geq 13.8 + 1.5 + 4.5$ cm^{-2} = 19.8 cm^{-2}, very close to our first estimate. A low column density is consistent with that found by Briggs et al. (2000) from fitting a combined set of BATSE and *BeppoSAX* X-ray and gamma-ray data.

HST imaging, performed in 2000 April, appears to detect a very faint ($V \sim 28$) galaxy, located only 0.″08 east of the position of the early afterglow (Fruchter et al. 2000; Bloom et al. 2000). This galaxy is probably responsible for the detected absorption lines in the spectra. The type and strength of the absorption lines, which are indicative of a low-ionization, high-density medium, strongly suggest that these originate in the host galaxy of GRB 990510. Even though the galaxy is extremely faint, the GRB afterglow allows us to probe its interstellar medium and—in principle—to measure its metallicity. For the latter we need a measure of the column density that does not depend on the strength of the metal absorption lines (e.g., from a Balmer feature).

4. THE EMISSION- AND ABSORPTION-LINE SPECTRUM OF GRB 990712

Figure 2 shows the spectra of GRB 990712, taken at 0.5, 0.7, and 1.5 days after the burst (see Table 1). The obvious emission lines are easily identified as [O II] λ3727, [Ne III] λ3869, Hγ, Hδ, and [O III] $\lambda\lambda$4959, 5007. We also detect two absorption lines, which can be identified as Mg II $\lambda\lambda$2796, 2804 and Mg I λ2853 at the same redshift as the emission lines, and are therefore intrinsic to the host galaxy. Using all these features in all three spectra, we obtain a weighted average redshift of $z = 0.4331 \pm 0.0004$. In Table 3 we list the observed wavelength of the features, their identification and redshift, and the rest-frame EW and flux (corrected for the Galactic foreground extinction), for the spectra taken at different epochs. The last two columns contain the EW and flux values averaged over all the spectra.

It is important to investigate whether GRB host galaxies are indeed star-forming galaxies, i.e., H II galaxies, where massive O and B stars ionize the interstellar medium, giving rise to prominent emission lines. These lines are also observed in galaxies that host an active galactic nucleus (AGN) (e.g., Seyfert 2), where their strength does not depend only on the star formation, but on the nuclear activity as

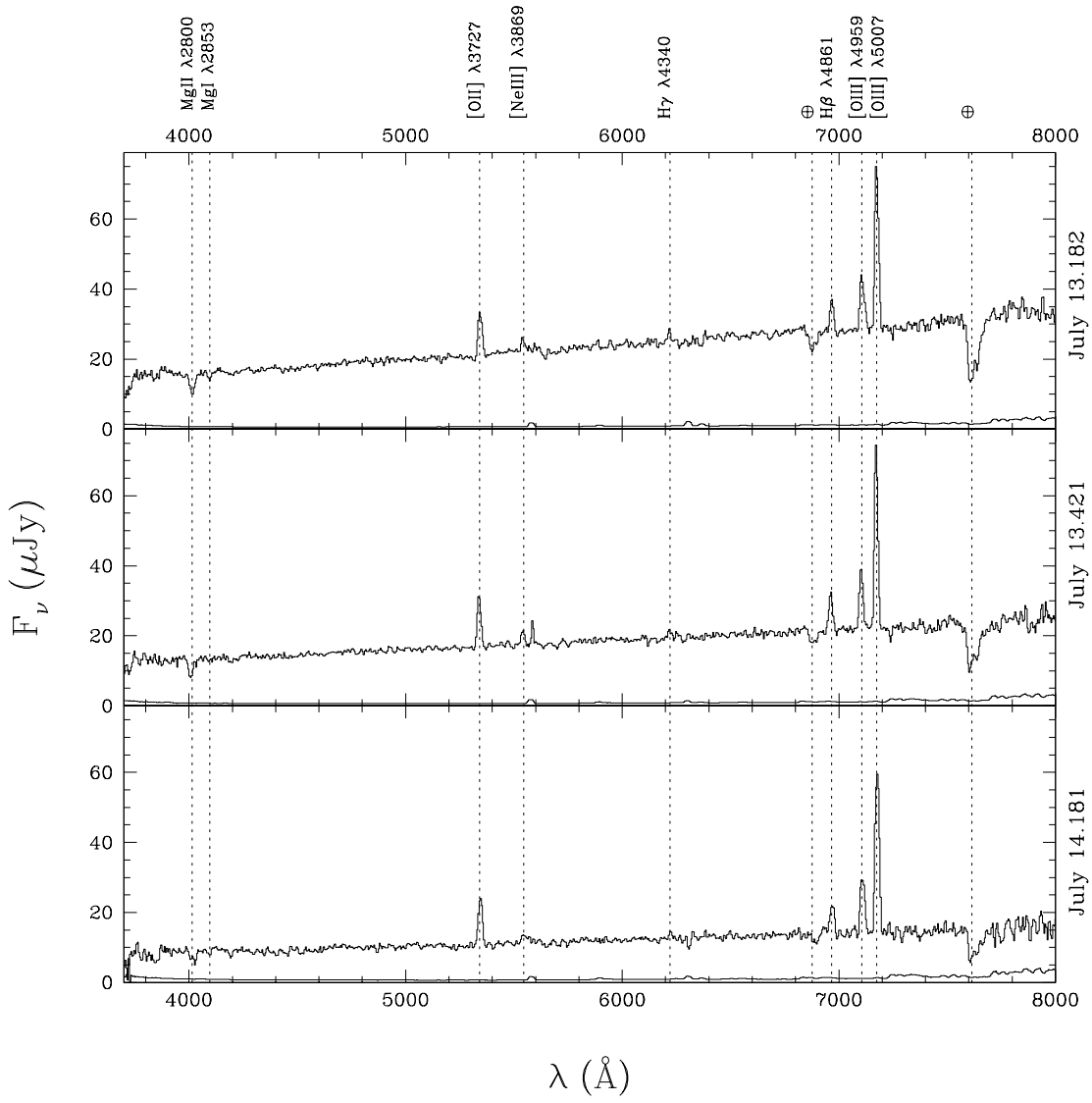

FIG. 2.—VLT/FORS1 spectra of the afterglow of GRB 990712, from 0.5 to 1.5 days after the burst. The error spectra, calculated from the object and sky spectra using Poisson statistics, are also shown. The absorption features (including telluric lines marked with ⊕) and emission features are indicated with the broken lines. The observation dates (also shown in the figure), grisms, resolving power, and signal-to-noise ratios are listed in Table 1 .

well. Most popular GRB progenitor models require a close connection with massive-star formation, but so far this has not been confirmed for any of the host galaxies.

Hjorth et al. (2000) suggested that the host galaxy of GRB 990712 may be a Seyfert 2 galaxy on the basis of the [O III] λ5007/Hβ ratio being greater than 3 (see Shuder & Osterbrock 1981) and its location in the log ([O III] λ5007/Hβ) versus log ([O II]/[O III] λ5007) diagram (see Fig. 2 of Baldwin, Phillips, & Terlevich 1981). We also measure a ratio of [O III] λ5007/Hβ that is greater than 3: 4.6 ± 1.0. However, from the more recent work of Rola, Terlevich, & Terlevich (1997), who employ the Canada-France Redshift Survey (CFRS) sample of emission-line galaxies at redshifts $0 < z \leq 0.3$, it is clear that a value of 4.6 is actually very typical for H II galaxies (see their Fig. 1). Combined with our value for log ([O II]/Hβ) of 0.4 ± 0.1, the host of GRB 990712 is located clearly within the H II galaxy regime. We note that this diagram is corrected for extinction intrinsic to the distant galaxies, while the values in our Table 3 are not. However, the [O III] λ5007/Hβ ratio is only slightly affected by reddening. Rola et al. (1997) also build non–extinction-corrected diagrams to distinguish between H II galaxies and other emission-line galaxies; in all but one of these, where its location is on the border of the H II galaxy and Seyfert 2 regimes, the host galaxy of GRB 990712 is classified as an H II galaxy (e.g., Table 3 gives $C_{3727} - C_{4861} = -0.28 \pm 0.03$, whereas Fig. 4 of Rola et al. 1997 shows all definite Seyfert 2s have $C_{3727} - C_{4861} > 0.4$); i.e., the emission lines are produced by H II regions that are being ionized by O and B stars. We conclude GRB 990712 is most likely an H II galaxy, and not a Seyfert 2.

We have estimated the host galaxy extinction, by comparing the observed ratio of Hγ/Hβ (0.26 ± 0.09) with the expected ratio for case B recombination (0.469 ± 0.009; Osterbrock 1989). Using the Galactic extinction curve of Cardelli et al. (1989), we obtain $A_V = 3.4^{+2.4}_{-1.7}$. The relative large error is due to the marginal detection of Hγ.

We can now estimate the star formation rate (SFR) in the host galaxy of GRB 990712 in three different ways: through the [O II] and Hβ line luminosities (Kennicutt 1998) and

TABLE 3

ABSORPTION AND EMISSION LINES IN GRB 990712

			JULY 13.18		JULY 13.42		JULY 14.18		WEIGHTED MEAN	
λ_{obs} (Å)	IDENTIFICATION	z	$W_{\lambda_{rest}}$ (Å)	Line Flux	$W_{\lambda_{rest}}$ (Å)	Line Flux	$W_{\lambda_{rest}}$ (Å)	Line Flux	$W_{\lambda,rest}$	Line Flux
4015 ± 6	Mg II $\lambda\lambda$2796, 2804	0.4340 ± 0.0021	8.3 ± 1.4		9.7 ± 1.9		13.7 ± 4.5		9.1 ± 1.3	
4096 ± 6	Mg I λ2853	0.4357 ± 0.0021	2.2 ± 0.6		<2 (2σ)		3.9 ± 1.4		2.5 ± 0.7	
5342 ± 3	[O II] λ3727	0.4332 ± 0.0008	-47.1 ± 7.4	3.27 ± 0.20	-44.7 ± 7.9	3.33 ± 0.22	-45.8 ± 8.6	3.37 ± 0.33	-45.9 ± 1.2	3.32 ± 0.14
5545 ± 5	[Ne III] λ3869	0.4332 ± 0.0013	-8.4 ± 1.5	0.60 ± 0.08	-10.9 ± 2.3	0.79 ± 0.11	-7.5 ± 1.9	0.55 ± 0.11	-8.6 ± 1.2	0.63 ± 0.10
6220 ± 3	Hγ λ4340	0.4332 ± 0.0007	-8.1 ± 3.3	0.50 ± 0.18	-6.0 ± 2.5	0.39 ± 0.14	-4.5 ± 1.8	0.29 ± 0.10	-5.5 ± 1.3	0.35 ± 0.11
6966 ± 3	Hβ λ4861	0.4330 ± 0.0006	-21.1 ± 3.9	1.17 ± 0.12	-28.6 ± 5.3	1.59 ± 0.17	-22.4 ± 7.7	1.23 ± 0.31	-23.5 ± 3.5	1.33 ± 0.20
7106 ± 3	[O III] λ4959	0.4330 ± 0.0006	-43.7 ± 7.0	2.36 ± 0.18	-40.7 ± 6.2	2.28 ± 0.16	-42.8 ± 8.8	2.38 ± 0.30	-42.2 ± 1.5	2.32 ± 0.12
7175 ± 2	[O III] λ5007	0.4330 ± 0.0004	-113.5 ± 17.1	6.04 ± 0.31	-110.7 ± 15.1	6.15 ± 0.25	-108.0 ± 18.6	6.18 ± 0.53	-110.9 ± 10.2	6.14 ± 0.19
Weighted mean:...		0.4331 ± 0.0004								

NOTES.—All flux units: 10^{-16} ergs s^{-1} cm^{-2}. All line fluxes have been corrected for the Galactic foreground extinction.

through the continuum flux at 2800 Å (Madau, Pozzetti, & Dickinson 1998). For all these estimates a Salpeter initial mass function (IMF) has been assumed. Combining equation (3) of Kennicutt (1998), a luminosity distance of 6.8×10^{27} cm (taking $H_0 = 70$ km s^{-1} Mpc^{-1}, $\Omega_0 = 0.3$, and $\Lambda = 0$), and the [O II] λ3727 line flux from Table 3 (the fluxes in this table have already been corrected for Galactic extinction), we obtain SFR([O II]) $= 2.7 \pm 0.8\ M_\odot\ \mathrm{yr}^{-1}$, consistent with the value found by Hjorth et al. (2000). Taking into account the measured extinction (at Hα, due to the fact that the [O II] SFR method is calibrated through Hα), using the Galactic extinction curve (Cardelli et al. 1989), we find SFR([O II]) $= 35^{+178}_{-25}\ M_\odot\ \mathrm{yr}^{-1}$. Using equation (2) of Kennicutt (1998), the case B (large optical depth) line ratio $j_{\mathrm{H}\alpha}/j_{\mathrm{H}\beta}$ of 2.85 (Osterbrock 1989) and the Hβ flux of Table 3, we find SFR(Hβ) $= 1.7 \pm 0.6\ M_\odot\ \mathrm{yr}^{-1}$. Corrected for reddening, this becomes SFR(Hβ) $= 64^{+770}_{-54}$ $M_\odot\ \mathrm{yr}^{-1}$. Finally, equation (2) of Madau et al. (1998), combined with the 2800 Å flux (which is located at 4013 Å at a redshift of 0.4331), gives SFR(2800 Å) $= 2.8 \pm 0.9\ M_\odot\ \mathrm{yr}^{-1}$, which becomes $\sim 400\ M_\odot\ \mathrm{yr}^{-1}$, using $A_V = 3.4$. The [O II] method, although it is indirectly calibrated through Hα and sensitive to the abundance and ionization state of the gas, is probably the least uncertain of the three. The Hβ estimate is uncertain due to the unknown host galaxy stellar absorption underneath the emission. The SFR based on the ultraviolet continuum is very uncertain due to the fact that our flux calibration is an extrapolation below the V band, and more importantly the extinction correction at ultraviolet wavelengths is very uncertain. Normally, the 2800 Å SFR is found to be lower by a factor of 2–3 (at redshifts up to $z = 2.8$) as compared to the Hα luminosity SFR method (Glazebrook et al. 1999; Yan et al. 1999).

For the GRB host galaxies for which an SFR has been determined so far, even for the [O II] method alone, the values range from $0.5 \pm 0.15\ M_\odot\ \mathrm{yr}^{-1}$ (GRB 970228; Djorgovski et al. 1999) to $20 \pm 9\ M_\odot\ \mathrm{yr}^{-1}$ (GRB 980703; Djorgovski et al. 1998); host galaxy extinction is not included, so these values should be considered as lower limits. Normalized by the host B-band luminosity, this range is narrowed down to spread a factor of 3. It has been noted (e.g., Djorgovski et al. 1998) that the range of SFRs for GRB host galaxies does not seem to be extraordinarily high, as compared to field galaxies at similar redshifts; e.g., Glazebrook et al. (1999) find a range of 20–60 $M_\odot\ \mathrm{yr}^{-1}$ (using Hα), for 13 field galaxies at $z = 1$, drawn from the CFRS. However, the galaxies at high redshifts for which these rates have been measured tend to be much brighter than the typical GRB host galaxy and are therefore expected to have much higher SFRs. The [O II] equivalent width, which effectively is the star formation rate normalized by the blue-band luminosity of the host galaxy, allows a more useful comparison. The mean W_{rest}([O II]) of the Glazebrook et al. sample is 33 ± 4 Å, while we measure W_{rest}([O II]) $= 46 \pm 1$ Å for the host of GRB 990712. This comparison also suggests that GRB 990712 occurred in a galaxy that is vigorously forming stars.

Using the oxygen and Hβ emission lines, we can estimate the global oxygen abundance of the host of GRB 990712 (see Kobulnicky, Kennicutt, & Pizagno 1999 and references therein). From the values in Table 3 we obtain $R_{23} \equiv (I_{3727} + I_{4959} + I_{5007})/\mathrm{H}\beta = 8.9 \pm 1.5$, corresponding to log (O/H) $= -3.7 \pm 0.4$ [we note that log $(\mathrm{O/H})_\odot = -3.1$; Allen & Cox 2000]. This estimate is based on fluxes not corrected for reddening, but such a correction would not change the abundance estimate substantially. For comparison, the oxygen abundances for a sample of 22 relatively nearby spiral galaxies range from log (O/H) $= -2.7$ to -3.5 (Kobulnicky et al. 1999).

5. THE TIME DEPENDENCE OF THE Mg II FEATURE

It is now well established that GRBs are the most energetic events in the universe, with peak isotropic luminosities up to 10^{53} ergs s^{-1} (Kulkarni et al. 1998). Also when the radiation from GRBs is beamed, the impact of the shock on the circumburst material is the same as in an isotropic explosion, and could be observable as time-resolved evolution of the Fe Kα line and edge in the X-ray regime (Weth et al. 2000 and references therein) and of ultraviolet absorption lines, redshifted to the optical domain (Perna & Loeb 1998). By monitoring the line evolution it is possible to obtain information on the density structure surrounding the explosion, and—in case the density can be measured by an independent method—the redshift to the burst may be obtained (Perna & Loeb 1998).

Our spectral observations of the afterglows of GRB 990510 and GRB 990712 extend over several nights, and both contain absorption lines, so that we can look for possible temporal evolution of these features. They are expected to decrease in time, if a considerable fraction of the atoms responsible for the absorption are in the vicinity of the site of the burst, and are ionized by the explosion (Perna & Loeb 1998). Alternatively, the burst may release atoms that are locked in the dust, which could result in a corresponding increase of the EWs. The clearest absorption feature in both bursts is Mg II. In the May 11 and May 14 spectra of GRB 990510 (0.8 and 3.9 days after the burst, respectively), we measure $W_{\mathrm{rest}} = 2.6 \pm 0.4$ Å (May 11) and $W_{\mathrm{rest}} = 2.3 \pm 0.6$ Å (May 14). For GRB 990712 we obtain $W_{\mathrm{rest}} = 8.3 \pm 1.4$ Å, $W_{\mathrm{rest}} = 9.7 \pm 1.9$ Å, and $W_{\mathrm{rest}} = 13.7 \pm 4.5$ Å for 0.5, 0.7, and 1.5 days after the burst, respectively. For both bursts, the values are constant within the errors. This is not very surprising; the Mg II feature is most likely saturated in the spectra of both bursts. This means that over a wide range of column densities, the EW is not expected to change by a detectable amount. On the other hand, a significant change in the EW would have indicated a large change in the column density. The Mg I feature in GRB 990712, which is possibly saturated as well, is also constant within the errors.

6. CONCLUSIONS

GRB afterglows allow us to probe galaxies that would otherwise be extremely difficult or impossible to study spectroscopically. We have determined a lower limit to the redshift of GRB 990510 through identification of several spectral absorption lines. The strength of the Mg I line is indicative of a cool, dense environment, which leads to the conclusion that the measured $z = 1.6187 \pm 0.0015$ most likely reflects absorption in the host galaxy ISM.

Using both the absorption and emission lines in the spectrum of GRB 990712, we determine its redshift at $z = 0.4331 \pm 0.0004$. The emission-line ratios indicate that the host of GRB 990712 is an H II galaxy, with an [O II] star formation rate (reddening corrected) of $35^{+178}_{-25}\ M_\odot\ \mathrm{yr}^{-1}$. The large [O II] equivalent width, compared to that of field galaxies at $z \leq 1$, also suggests that the host is vigorously forming stars.

In order to put meaningful constraints on the circumsource medium, high-resolution, high signal-to-noise spectra at several epochs after the burst are needed to resolve the velocity structures of the nonsaturated lines and allow determination of the circumsource density distribution and its evolution. This may become possible with the launch of *HETE-2*, since this satellite will allow follow-up observations of optical transients at early times, i.e., when they are bright ($R \sim 16$). Determination of the density profile could provide a major advance in solving the progenitor problem.

P. M. V. and E. R. are supported by the NWO Spinoza grant. C. K. acknowledges support from NASA grant NAG 5-2560. T. J. G. acknowledges support from the Sherman Fairchild Foundation. L. K. is supported by a fellowship of the Royal Academy of Sciences of the Netherlands. We especially want to thank the ESO/VLT staff on Cerro Paranal who performed most of the TOO observations and assisted us during the nights of FORS Consortium guaranteed time.

REFERENCES

Allen, C. W., & Cox, A. N. 2000, Allen's Astrophysical Quantities (4th ed.; New York: AIP)
Bakos, G., et al. 1999, IAU Circ. 7225
Baldwin, J. A., Phillips, M. M., & Terlevich, R. 1981, PASP, 93, 5
Beuermann, K., et al. 1999, A&A, 352, L26
Bloom, J., et al. 2000, GCN Circ. 756 (http://gcn.gsfc.nasa.gov.gcn/gcn3/756.gcn3)
Briggs, M. S., et al. 2000, in AIP Conf. Proc. 526, Gamma-Ray Bursts: Fifth Huntsville Symp., ed. R. M. Kippen, R. Mallozzi, & G. Fishman (New York: AIP), 125
Cardelli, J. A., Clayton, G. C., & Mathis, J. S. 1989, ApJ, 345, 245
Costa, E., et al. 1997, Nature, 387, 783
Covino, S., et al. 1999, A&A, 348, L1
Dadina, M., et al. 1999, IAU Circ. 7160
Djorgovski, S. G., et al. 1998, ApJ, 508, L17
———. 1999, GCN Circ. 289 (http://gcn.gsfc.nasa.gov.gcn/gcn3/289.gcn3)
Fruchter, A., et al. 1999, GCN Circ. 386 (http://gcn.gsfc.nasa.gov.gcn/gcn3/386.gcn3)
———. 2000, GCN Circ. 757 (http://gcn.gsfc.nasa.gov.gcn/gcn3/757.gcn3)
Fukugita, M., Shimasaku, K., & Ichikawa, T. 1995, PASP, 107, 945
Galama, T. J., et al. 1998, Nature, 395, 670
———. 1999, GCN Circ. 388 (http://gcn.gsfc.nasa.gov.gcn/gcn3/388.gcn3)
Glazebrook, K., et al. 1999, MNRAS, 306, 843
Grevesse, N., & Sauval, A. J. 1999, A&A, 347, 348
Hansen, B. M. S., & Phinney, E. S. 1997, MNRAS, 291, 569
Harrison, F. A., et al. 1999, ApJ, 523, L121
Heise, J., et al. 1999, IAU Circ. 7221
Hjorth, J., et al. 2000, ApJ, 534, L147 (erratum 539, L75)
Hurley, K., et al. 1999, GCN Circ. 309 (http://gcn.gsfc.nasa.gov.gcn/gcn3/309.gcn3)
Janka, H.-T., Eberl, T., Ruffert, M., & Fryer, C. L. 1999, ApJ, 527, L39
Jenkins, E. B., & Wallerstein, G. 1995, ApJ, 440, 227
Kennicutt, R. C. 1998, ARA&A, 36, 189
Kippen, R. M., et al. 1999, GCN Circ. 322 (http://gcn.gsfc.nasa.gov.gcn/gcn3/322.gcn3)
Kobulnicky, H. A., Kennicutt, R. C., & Pizagno, J. L. 1999, ApJ, 514, 544
Kulkarni, S. R., et al. 1998, Nature, 393, 35
MacFadyen, A. I., & Woosley, S. E. 1999, ApJ, 524, 262
Madau, P., Pozzetti, L., & Dickinson, M. 1998, ApJ, 498, 106
Mészáros, P. 2000, in Proc. 19th Texas Symposium on Relativistic Astrophysics and Cosmology, ed. E. Aubourg, T. Montmerle, J. Paul, & P. Peter (Amsterdam: North-Holland), 63
Morton, D. C. 1991, ApJS, 77, 119
Narayan, R., Paczyński, B., & Piran, T. 1992, ApJ, 395, L83
Osterbrock, D. E. 1989, Astrophysics of Gaseous Nebulae and Active Galactic Nuclei (Mill Valley: University Science Books)
Perna, R., & Loeb, A. 1998, ApJ, 501, 467
Pettini, M., et al. 1997, ApJ, 486, 665
Piran, T. 1999, Phys. Rep., 314, 575
Portegies Zwart, S. F., & Yungelson, L. R. 1998, A&A, 332, 173
Rol, E., et al. 2000, ApJ, 544, 707
Rola, C. S., Terlevich, E., & Terlevich, R. J. 1997, MNRAS, 289, 419
Sahu, K., et al. 2000, ApJ, 540, 74
Savage, B. D., & Sembach, K. R. 1996, ARA&A, 34, 279
Schlegel, D. J., Finkbeiner, D. P., & Davis, M. 1998, ApJ, 500, 525
Sembach, K. R., & Savage, B. D. 1996, ApJ, 457, 211
Shuder, J. M., & Osterbrock, D. E. 1981, ApJ, 250, 55
Spitzer, L. 1978, Physical Processes in the Interstellar Medium (New York: Wiley)
Stanek, K. Z., et al. 1999, ApJ, 522, L39
van Paradijs, J., et al. 1997, Nature, 386, 686
van Paradijs, J., Kouveliotou, C., & Wijers, R. A. M. J. 2000, ARA&A, 38, 379
Vreeswijk, P. M., et al. 1999, GCN Circ. 310 (http://gcn.gsfc.nasa.gov.gcn/gcn3/310.gcn3)
Weth, C., et al. 2000, ApJ, 534, 581
Whittet, D. C. B. 1992, Dust in the Galactic Environment (New York: Institute of Physics)
Wijers, R. A. M. J., et al. 1999, ApJ, 523, L33
Woosley, S. E. 1993, ApJ, 405, 273
Yan, L., et al. 1999, ApJ, 519, L47